

Generating few-cycle pulses for nanoscale photoemission easily with an erbium-doped fiber laser

Sebastian Thomas,^{1,*} Ronald Holzwarth,^{1,2} and Peter Hommelhoff¹

¹Max-Planck-Institut für Quantenoptik, Hans-Kopfermann-Str. 1, 85748 Garching, Germany

²Menlo Systems GmbH, 82152 Martinsried, Germany

*sebastian.thomas@mpq.mpg.de

Abstract: We demonstrate a simple setup capable of generating four-cycle pulses at a center wavelength of 1700 nm for nanoscale photoemission. Pulses from an amplified erbium-doped fiber laser are spectrally broadened by propagation through a highly non-linear fiber. Subsequently, we exploit dispersion in two different types of glass to compress the pulses. The pulse length is estimated by measuring an interferometric autocorrelation trace and comparing it to a numerical simulation. We demonstrate highly non-linear photoemission of electrons from a nanometric tungsten tip in a hitherto unexplored pulse parameter range.

© 2012 Optical Society of America

OCIS codes: (060.4370) Nonlinear optics, fibers; (140.3500) Lasers, erbium; (140.7090) Ultrafast lasers; (240.6675) Surface photoemission and photoelectron spectroscopy; (320.5520) Pulse compression; (320.6629) Supercontinuum generation.

References and links

1. J. D. Kafka, T. Baer, and D. W. Hall, "Mode-locked erbium-doped fiber laser with soliton pulse shaping," *Opt. Lett.* **14**, 1269–1271 (1989).
2. K. Tamura, E. P. Ippen, H. A. Haus, and L. E. Nelson, "77-fs pulse generation from a stretched-pulse mode-locked all-fiber ring laser," *Opt. Lett.* **18**, 1080–1082 (1993).
3. A. Sell, G. Krauss, R. Scheu, R. Huber, and A. Leitenstorfer, "8-fs pulses from a compact Er:fiber system: quantitative modeling and experimental implementation," *Opt. Express* **17**, 1070–1077 (2009).
4. A. Andrianov, A. Kim, S. Muravyov, and A. Sysoliatin, "Wavelength-tunable few-cycle optical pulses directly from an all-fiber er-doped laser setup," *Opt. Lett.* **34**, 3193–3195 (2009).
5. E. Anashkina, A. Andrianov, S. Muravyev, and A. Kim, "All-fiber design of erbium-doped laser system for tunable two-cycle pulse generation," *Opt. Express* **19**, 20141–20150 (2011).
6. G. Krauss, S. Lohss, T. Hanke, A. Sell, S. Eggert, R. Huber, and A. Leitenstorfer, "Synthesis of a single cycle of light with compact erbium-doped fibre technology," *Nat. Photon.* **4**, 33–36 (2010).
7. P. Hommelhoff, C. Kealhofer, and M. A. Kasevich, "Ultrafast electron pulses from a tungsten tip triggered by low-power femtosecond laser pulses," *Phys. Rev. Lett.* **97**, 247402 (2006).
8. P. Hommelhoff, Y. Sortais, A. Aghajani-Talesh, and M. A. Kasevich, "Field emission tip as a nanometer source of free electron femtosecond pulses," *Phys. Rev. Lett.* **96**, 077401 (2006).
9. C. Ropers, D. R. Solli, C. P. Schulz, C. Lienau, and T. Elsaesser, "Localized multiphoton emission of femtosecond electron pulses from metal nanotips," *Phys. Rev. Lett.* **98**, 043907 (2007).
10. M. Schenk, M. Krüger, and P. Hommelhoff, "Strong-field above-threshold photoemission from sharp metal tips," *Phys. Rev. Lett.* **105**, 257601 (2010).
11. R. Bormann, M. Gulde, A. Weismann, S. V. Yalunin, and C. Ropers, "Tip-enhanced strong-field photoemission," *Phys. Rev. Lett.* **105**, 147601 (2010).
12. M. Krüger, M. Schenk, M. Förster, and P. Hommelhoff, "Attosecond physics in photoemission from a metal nanotip," *J. Phys. B* **45**, 074006 (2012).
13. G. Wachter, C. Lemell, J. Burgdörfer, M. Schenk, M. Krüger, and P. Hommelhoff, "Electron rescattering at metal nanotips induced by ultrashort laser pulses," submitted, [arXiv:1201.0462](https://arxiv.org/abs/1201.0462) (2012).

14. M. Krüger, M. Schenk, and P. Hommelhoff, "Attosecond control of electrons emitted from a nanoscale metal tip," *Nature* **475**, 78–81 (2011).
15. G. Krauss, D. Fehrenbacher, D. Brida, C. Riek, A. Sell, R. Huber, and A. Leitenstorfer, "All-passive phase locking of a compact Er:fiber laser system," *Opt. Lett.* **36**, 540–542 (2011).
16. C. Homann, M. Bradler, M. Förster, P. Hommelhoff, and E. Riedle, "Carrier-envelope phase stable sub-two-cycle pulses tunable around 1.8 μm at 100 kHz," *Opt. Lett.* **37**, 1673–1675 (2012).
17. T. Hanke, G. Krauss, D. Träutlein, B. Wild, R. Bratschitsch, and A. Leitenstorfer, "Efficient nonlinear light emission of single gold optical antennas driven by few-cycle near-infrared pulses," *Phys. Rev. Lett.* **103**, 257404 (2009).
18. T. Hanke, J. Cesar, V. Knittel, A. Trügler, U. Hohenester, A. Leitenstorfer, and R. Bratschitsch, "Tailoring spatiotemporal light confinement in single plasmonic nanoantennas," *Nano Lett.* **12**, 992–996 (2012).
19. G. Herink, D. R. Solli, M. Gulde, and C. Ropers, "Field-driven photoemission from nanostructures quenches the quiver motion," *Nature* **483**, 190–193 (2012).
20. SchottAG, "Optical glass data sheets," http://www.us.schott.com/advanced_optics/english/download/schott_optical_glass_collection_datasheets_dec_2011_us.pdf.
21. R. Gomer, *Field Emission and Field Ionization* (Harvard University Press, 1961).
22. H. Kawano, "Effective work functions for ionic and electronic emissions from mono- and polycrystalline surfaces," *Prog. Surf. Sci.* **83**, 1–165 (2008).

1. Introduction

Femtosecond laser pulses with durations of just a few optical cycles are being used for a large number of applications including pump-probe spectroscopy, non-linear optics, high harmonic generation, and frequency measurements. Accordingly, there is a considerable interest in the generation of few-cycle laser pulses at different wavelengths. In the near-infrared regime, one source of femtosecond laser pulses are erbium-doped fiber lasers, introduced over twenty years ago [1,2]. However, they cannot generate few-cycle pulses directly due to the limited gain bandwidth of erbium-doped fibers. Recently, few- and even single-cycle pulses were created based on rather intricate erbium-doped fiber technology by exploiting non-linear effects in custom optical fibers to broaden the pulses' spectrum [3–5] and, in the case of the single-cycle pulse, by an interferometric technique [6].

Theoretical investigations have shown that spectral broadening in a highly non-linear fiber, which can be modeled as the combined effect of dispersion, an instantaneous Kerr response, and a retarded Raman response, leads to a separation of the spectrum into a long- and a short-wavelength part [3,5]. Based on this phenomenon, Sell et al. have demonstrated the generation of 8 fs pulses using only the short-wavelength part of the spectrum [3], Anashkina et al. have created 13 fs pulses by compressing a less broad and not completely separated spectrum generated in a short non-linear fiber [5], and Krauss et al. have succeeded in generating a single-cycle pulse by individually compressing and then recombining both parts of the spectrum [6]. All experiments relied on complex setups or optimized, dispersion-shifted fibers.

In this article, we present a similar yet particularly simple scheme to create few-cycle pulses, which uses only the long-wavelength part of spectrally broadened pulses from an erbium-doped fiber laser. Our setup consists entirely of standard commercial components and does not employ a customized non-linear fiber. Using only the long-wavelength part of the spectrum reduces the requirements on experimental components and allows us to compensate the spectral phase by exploiting quadratic dispersion in bulk glass. This enables us to compress the pulses to approximately 23 fs, corresponding to 4.1 optical cycles.

We employ the few-cycle pulses to study photoemission of electrons from sharp metal tips. A nanometric metal tip under laser illumination constitutes a localized electron source with a small emission area that is given by the extent of the enhanced optical near-field induced at the tip apex [7–9]. Such experiments have recently reached the strong-field regime [10–12], demonstrating phenomena like electron rescattering [13] and an emission current that depends on the pulses' carrier-envelope phase [14]. While most previous experiments in this area have

been carried out with Ti:sapphire lasers, going to longer wavelengths changes the dynamics of electron rescattering, modifies the initial emission process via the Keldysh parameter and leads to different material properties of the tip. As a first application of the laser setup, we demonstrate multiphoton photoemission from a tungsten tip triggered by the few-cycle infrared pulses.

Our results demonstrate that photoemission of electrons from sharp metal tips can be investigated with erbium-doped fiber technology. In the future, similar experiments may benefit from passive carrier-envelope phase stability [15, 16]. Spectrally broadened pulses from an erbium-doped fiber laser have previously been used to study second and third harmonic generation as well as plasmon response times at nanoantennas [17, 18]. Very recently, photoemission of electrons from metal tips has been investigated for a wide range of infrared wavelengths using a kilohertz system based on optical parametric amplification and difference frequency generation [19].

2. Experimental setup

An outline of the experimental setup is depicted in Fig. 1(a). The pulses are generated in a passively mode-locked erbium-doped fiber laser and amplifier (Menlo Systems C-Fiber A). The laser is mode-locked by non-linear polarization evolution. The parameters of the laser system, including the general shape of the spectrum, can be significantly varied by changing the configuration of the wave plates inside the oscillator. Typically, one obtains pulse durations of $\tau = 60$ to 90 fs (full width at half maximum of the intensity) with an average output power P of up to 400 mW and a repetition rate of $f_{\text{rep}} = 100$ MHz.

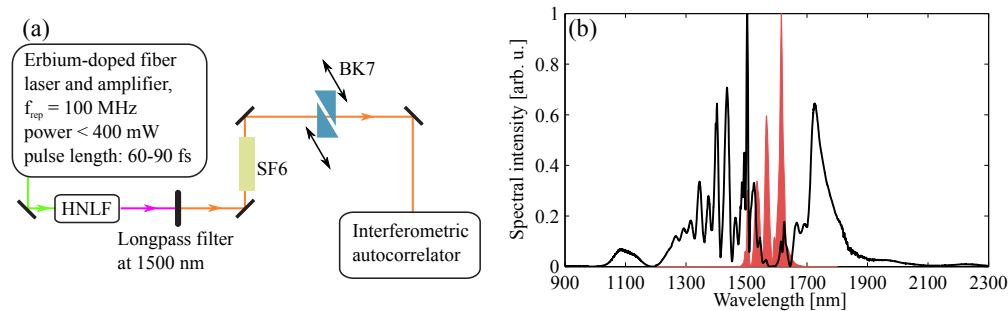


Fig. 1. (a) Outline of the experimental setup: pulses are generated in an erbium-doped fiber laser and spectrally broadened in a highly non-linear fiber (HNLF), the short-wavelength part of the spectrum is filtered out, the spectral phase is flattened using dispersion in glass, and the pulse duration is characterized in an autocorrelator. (b) Spectral intensity before (shaded red area) and after spectral broadening (black line) in the HNLF; shown here is a combination of measurements with two spectrum analyzers: Ando AQ6315E and Yokogawa AQ6375.

The beam is coupled into a highly non-linear fiber (Furukawa Electric OFS HNLF Standard) via an aspheric lens with a focal length of 1.49 mm (Thorlabs C710TME-C). The fiber is approximately 3.5 cm long with a typical effective area of $A_{\text{eff}} = 11.7 \mu\text{m}^2$, a zero-dispersion wavelength of $\lambda_0 = 1550$ nm, and a typical non-linear coefficient of $\gamma = 2\pi n_2 / \lambda_0 A_{\text{eff}} = 11.5 \text{W}^{-1} \text{km}^{-1}$, where n_2 is the second-order non-linear refractive index. The results of the spectral broadening due to the propagation through the fiber are shown in Fig. 1(b). The resulting spectrum may span a range between 1000 and 2300 nm depending on the parameters of the initial pulses.

After being coupled out of the fiber via another aspheric lens with 11 mm focal length (ThorLabs A397TM-C), the beam passes an 1500 nm interferometric longpass filter (Thorlabs FEL1500), which cuts off the short-wavelength part of the spectrum. It should be noted that the short-wavelength part supports pulse durations of less than 10 fs and may also be used to generate few-cycle pulses [3]. In order to compensate the spectral phase of the resulting pulses (i.e. of the long-wavelength components of the spectrum), we use quadratic dispersion in different types of glass: a small number of SF6 rods of different lengths (1.2 to 4.8 cm) and a closely-positioned BK7 prism pair, which can be adjusted to fine-tune the amount of glass in the beam (0.6 to 2.2 cm BK7 path length). The dispersion coefficients $D_n = d^n k/d\omega^n$ of these types of glass in the relevant spectral range from 1400 to 2000 nm can be obtained from Ref. [20] and are approximately: $D_2 \in [-200, 800] \text{ fs}^2/\text{cm}$, $D_3 \in [1500, 4000] \text{ fs}^3/\text{cm}$, $D_4 \in [-15000, -2000] \text{ fs}^4/\text{cm}$ for SF6 and $D_2 \in [-1000, -100] \text{ fs}^2/\text{cm}$, $D_3 \in [1000, 4500] \text{ fs}^3/\text{cm}$, $D_4 \in [-20000, -3000] \text{ fs}^4/\text{cm}$ for BK7. SF6 has positive second-order dispersion for wavelengths up to approximately 1900 nm while BK7 has negative second-order dispersion for wavelengths greater than 1350 nm. Note that a longpass filter blocking the residual components of the driving pulse around 1550 nm might be advantageous for obtaining short pulses.

We use a Michelson type interferometric autocorrelator with a thin pellicle beam splitter to characterize the pulse duration. A silicon photodiode serves as both second-order non-linear optical element and detector of the two-photon signal.

3. Results

The results depicted in Fig. 2 show a measurement of typical pulses produced in our setup. During this measurement, the beam passed SF6 rods of a total length of 6 cm and BK7 glass of a total length of 1 cm. The average output power of the fiber laser was 235 mW before broadening in the HNLF and 171 mW after broadening (corresponding to a coupling efficiency of 73%). Figure 2(a) depicts the autocorrelation trace we measured after optimizing the amount of glass inside the beam to compensate the spectral phase. The spectrum of the pulses is shown in Fig. 2(c). It has a center wavelength of 1680 nm. In order to obtain the pulse duration, we compare the autocorrelation trace to simulations of the trace, which are based on the spectrum and assume a higher order spectral phase. Here, we find the best fit between measurement and simulation by assuming a fourth order phase. The simulated trace, the assumed spectral phase and the resulting temporal pulse shape are depicted in Fig. 2(b)–2(d).

The resulting pulse duration is $\tau = (23.1 \pm 1.5) \text{ fs}$. We obtained an estimate of the uncertainty by comparing simulated traces with different magnitudes of the spectral phase to the measured trace. The pulse duration is approximately 30% above the spectrum's Fourier limit of 17.7 fs. Using other types of glass might even help to reduce the pulse duration into the three-cycle regime, closer to the Fourier limit. Note that no double-chirped mirrors or prism compressors are needed to obtain this pulse duration. We hence expect this setup to be easily integrable into a fully fiber-based system, similar to Ref. [5].

While the measured and simulated autocorrelation traces agree very well in the center of the trace (for $|\text{delay}| < 400 \text{ fs}$) there is only a qualitative agreement for greater delays, where the simulation shows significantly smaller wings. This suggests that our simulation underestimates the amplitude of the satellite pulses. As the autocorrelation signal of these wings remains smaller than 2, the satellites are unlikely to change the pulse duration or to significantly contribute to the highly non-linear photoemission process we will discuss in the next section.

4. Multiphoton photoemission

As a first application of the laser system, we will present measurements of photoemission of electrons from a sharp tungsten tip. We focus the laser pulses onto the apex of a sharp tungsten

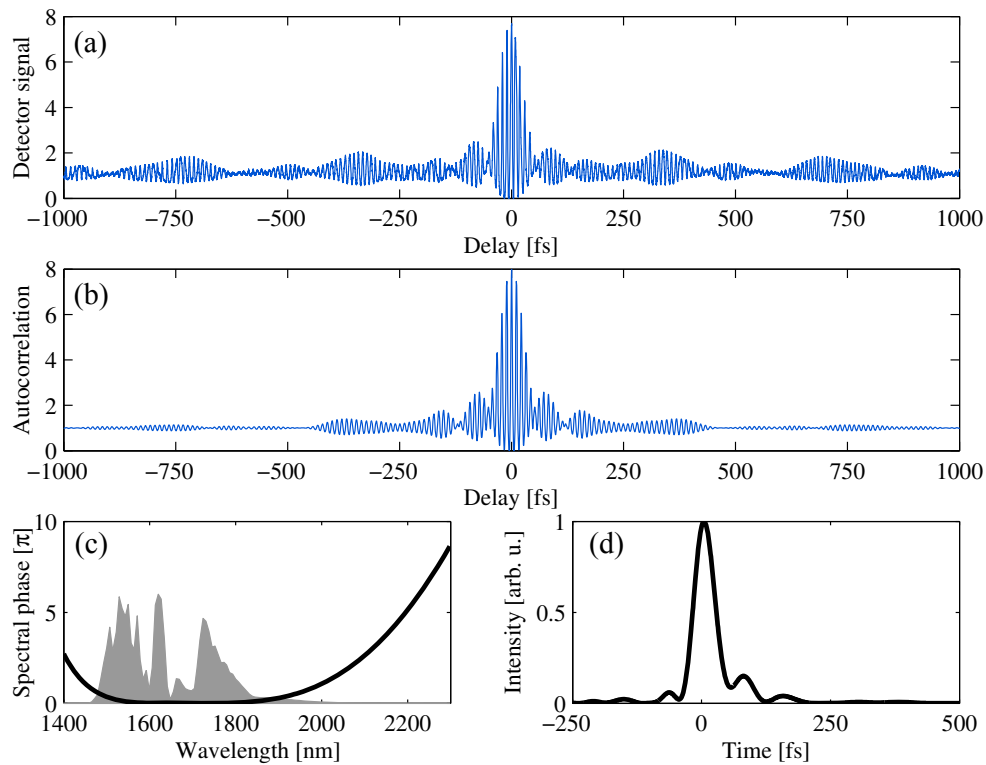


Fig. 2. (a) Measured autocorrelation trace; (b) simulated autocorrelation trace; (c) measured spectral intensity (gray area) and the assumed spectral phase (line) used in the simulation; (d) temporal pulse shape corresponding to (c).

tip using an off-axis parabolic mirror. The waist radius of the beam in the focus is approximately $6\ \mu\text{m}$ ($1/e^2$ of the intensity). The tip is made of (310)-monocrystalline tungsten wire and has a radius of curvature of around 10 nm. Both the tip and the mirror are arranged in an ultra-high vacuum chamber. In addition to the laser field, a static voltage can be applied to the tip. We measure the electron emission current from the tip using a micro-channel plate (MCP) detector. A more detailed description of the setup is given in Ref. [10].

In this setup, electrons are emitted from the tip surface via the absorption of multiple photons. The photon order of this process depends on the effective barrier height at the surface, which varies with the applied voltage due to the Schottky effect [21]. The effective barrier height is then given by the work function of the material decreased by $\Delta E = (e^3 F / 4\pi\epsilon_0)^{1/2}$. In this equation, e is the electron charge, ϵ_0 is the vacuum permittivity, and F is the static electric field at the surface. Figure 3 shows the potential for three different settings of the static voltage.

To determine the photon order in the experiment, we measure the electron emission current J while varying the average power P of the laser illuminating the tip. For an emission process of photon order n , J is proportional to P^n . Results of this measurement for two different electric fields $F = 2.2\ \text{GV/m}$ and $1.4\ \text{GV/m}$ at the tip are plotted in Fig. 4. We obtain the photon order by fitting a power law to the measured data.

The fit results suggest that we observe four- and five-photon absorption as the dominant emission process, respectively, which implies that the barrier height lies between 2.2 and 3.0 eV in the first and between 3.0 and 3.7 eV in the second case. Calculating the Schottky effect for

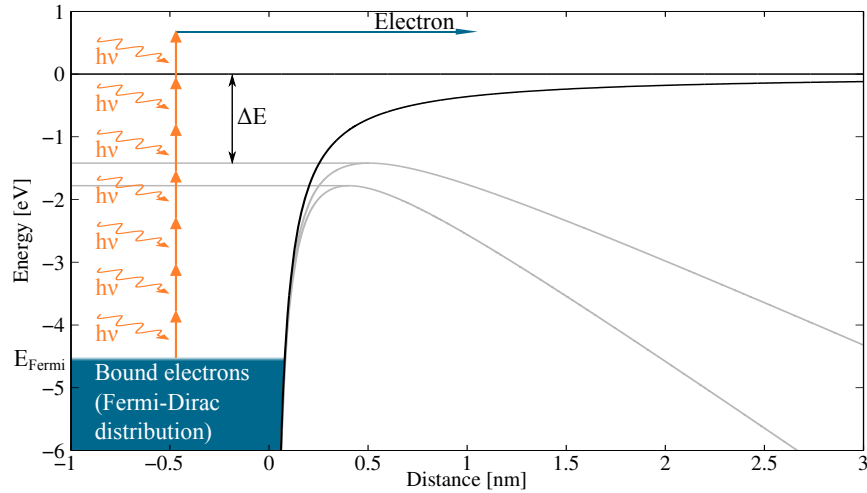


Fig. 3. Illustration of multiphoton absorption and the Schottky effect at a tungsten surface: in order to be emitted, an electron's energy must be raised from an energy $E \leq E_{\text{Fermi}}$ to the continuum $E \geq 0$. An additional static voltage at the surface lowers the barrier height, thus reducing the required energy. The barrier is plotted for zero voltage (black line) and for the voltages applied in the experiment, corresponding to fields of 2.2 (lower grey line) and 1.4 GV/m (upper grey line).

the two electric fields and combining the results with the effective barrier height, we find that the work function of the tungsten tip must be between 4.4 and 4.8 eV, which is consistent with previously published values for tungsten [22].

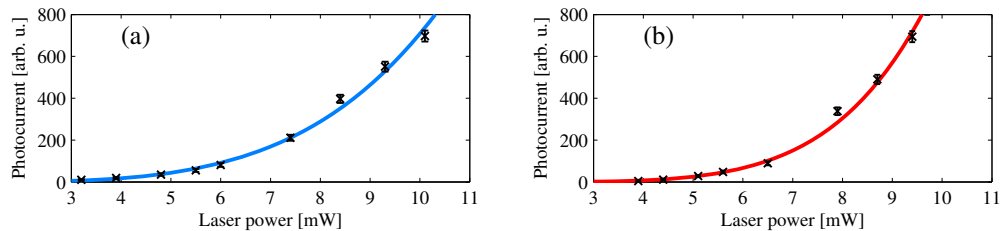


Fig. 4. Photocurrent J as function of laser power P for two different static electric fields; (a) $F = 2.2 \text{ GV/m}$, fit result: $J \sim P^{4.0 \pm 0.3}$; (b) $F = 1.4 \text{ GV/m}$, fit result: $J \sim P^{5.3 \pm 0.4}$.

5. Conclusion

We have presented a simple setup capable of generating four-cycle pulses at 1700 nm based on an amplified erbium-doped fiber laser and a commercial highly non-linear fiber. Our results show that exploiting group velocity dispersion in glass is sufficient to achieve pulse durations down to only four optical cycles. Additionally, we have shown results from photoemission experiments as a first application of our laser system, demonstrating the reliability of the setup.

Acknowledgments

We acknowledge the contribution of Yui-Hong Matthias Tan in the early stages of the experiment. We also thank the reviewers of this manuscript for their excellent technical comments.